JOC The Journal of Organic Chemistry

Article

pubs.acs.org/joc

Understanding the Reactivity and Regioselectivity of Methylation of Nitronates $[R^1R^2CNO_2]^-$ by CH_3I in the Gas Phase

Ayyaz Mahmood,* Erico Souza Teixeira, and Ricardo L. Longo*

Departamento de Química Fundamental, Universidade Federal de Pernambuco, Cidade Universitária, Recife, PE 50740-560, Brazil

Supporting Information

ABSTRACT: Methylation of $[R^1R^2CNO_2]^-$, where $R^1 = R^2 = H$ (**1**), $R^1 = CH_3$ and $R^2 = H$ (**2**), $R^1 = R^2 = CH_3$ (**3**), and $R^1 + R^2 =$ c-$(CH_2)_2$ (**4**), by CH_3I was studied by an *ab initio* MP2/CBS method, RRKM theory, and kinetic simulations. Contrary to a previous proposal for the reaction mechanism, C-methylation is the preferred pathway of thermodynamics and kinetics. This is corroborated by the agreement between the calculated and experimental reactivity trend **4** ≫ **3** > **2** > **1**. The regioselectivity toward C-alkylation is explained by the much larger exothermicity of this reaction channel compared to that of O-alkylation. The increase in reactivity with an increase in the crowdedness of the central carbon atom is explained by differences in sp^3 character at this atom and the decrease in the vibrational frequency associated with pyramidalization around this carbon atom.

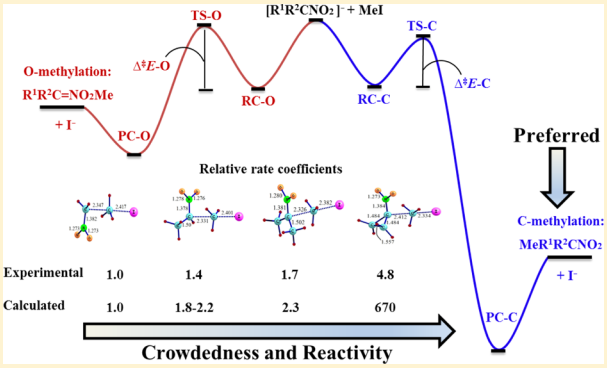

INTRODUCTION

Deprotonation of nitroalkanes, $R^1R^2CHNO_2$, can be achieved in the gas phase and in solution under mild and controlled conditions.[1−4] These generated anions, $[R^1R^2CNO_2]^-$, known as nitronates or azinates, are useful synthetic reactive intermediates because they can form C−C and/or C−O bonds.[1−8] For instance, the Henry (or nitro-aldol) reaction between nitronates and aldehydes or ketones is a classic carbon−carbon bond formation reaction.[1−9] Alkylations of nitronates are also quite useful reactions; however, the ambident nature of these anions[10] may lead to C-alkylation and O-alkylation.[1−9,11] Thus, determining the origin of the regioselectivity in alkylations of nitronates is important to broaden the scope of these reactions. For instance, only O-alkylated products were obtained in the reaction of ring-substituted phenylnitromethanes with MeOBs in several protic and aprotic solvents, where the stereoselectivity in X-Ph−CH═N(O)OMe always favored the *Z* isomer; however, the *Z*:*E* ratio was dependent on the solvent.[11] B3LYP/6-31+G* calculations for these reactions suggested a kinetic preference for O-methylations because they presented barriers lower than those of the respective C-methylations.[11] It is noteworthy that these and many other experimental studies were performed in solution, where the solvent can have significant effects that mask the intrinsic reactivity and selectivity.[12] In fact, the energy profiles of S_N2 reactions in the gas phase are quite different from those in solution,[12,13] which leads, for instance, to large differences between reaction rate constants.[14,15] In addition, there have been reports of reversal of ordering of acidities and basicities in solution compared to those in the gas phase and significant nucleophilicity differences in polarizable nucleophiles in solution and the gas phase.[16−18] Thus, studying reactions in the gas phase is relevant to determine the intrinsic reactivity and selectivity, which by comparisons with solution studies can be used to ascertain and, possibly, quantify the solvent effects. Indeed, reactions of alkyl-nitronates $[R^1R^2CNO_2]^-$, where $R^1 = R^2 = H$ (**1**), $R^1 = CH_3$ and $R^2 = H$ (**2**), $R^1 = R^2 = CH_3$ (**3**), and $R^1 + R^2 =$ c-$(CH_2)_2$ (**4**), with iodomethane (CH_3I), depicted in Scheme 1, were studied in the gas phase using the flowing afterglow technique.[19] The reaction with asymmetric nitronates, such as $[CH_3CHNO_2]^-$, can yield *Z* and *E* stereoisomers.

Scheme 1. Reactions of Alkyl-nitronates $[R^1R^2CNO_2]^-$, where $R^1 = R^2 = H$ (1), $R^1 = CH_3$ and $R^2 = H$ (2), $R^1 = R^2 = CH_3$ (3), and $R^1 + R^2 =$ c-$(CH_2)_2$ (4), with Iodomethane (CH_3I)[a]

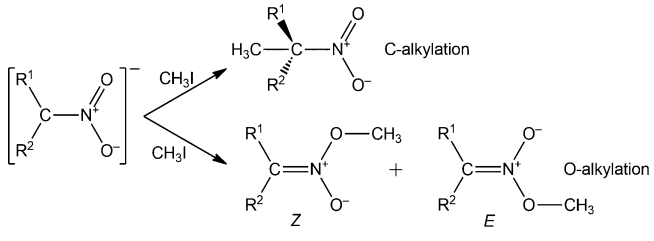

[a]For asymmetric nitronates such as **2**, O-alkylation yields *Z* and *E* stereoisomers.

Received: June 5, 2015
Published: July 16, 2015

DOI: 10.1021/acs.joc.5b01273
J. Org. Chem. 2015, 80, 8198−8205

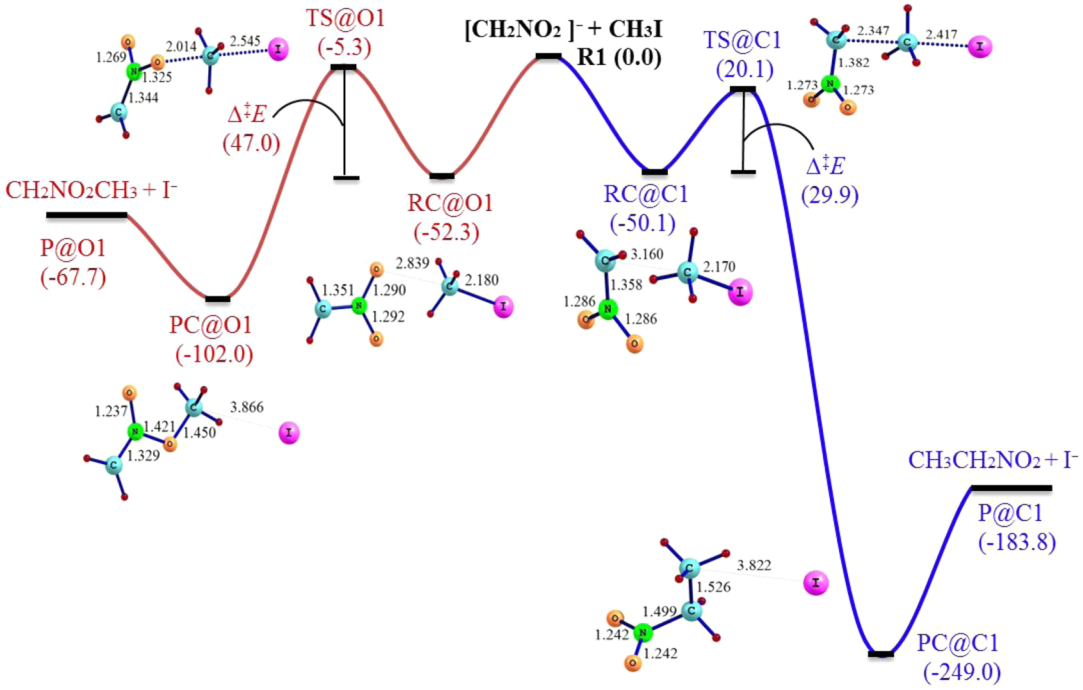

Figure 1. Energy profiles and selected structures of the $[CH_2NO_2]^-$ + CH_3I gas-phase reaction of **1** through the oxygen (S_N2@O), O-methylation, and the carbon (S_N2@C), C-methylation, atoms of the nucleophile. Calculations at the MP2/CBS level. Energies (in kilojoules per mole) include the zero-point vibrational corrections and distances in angstroms.

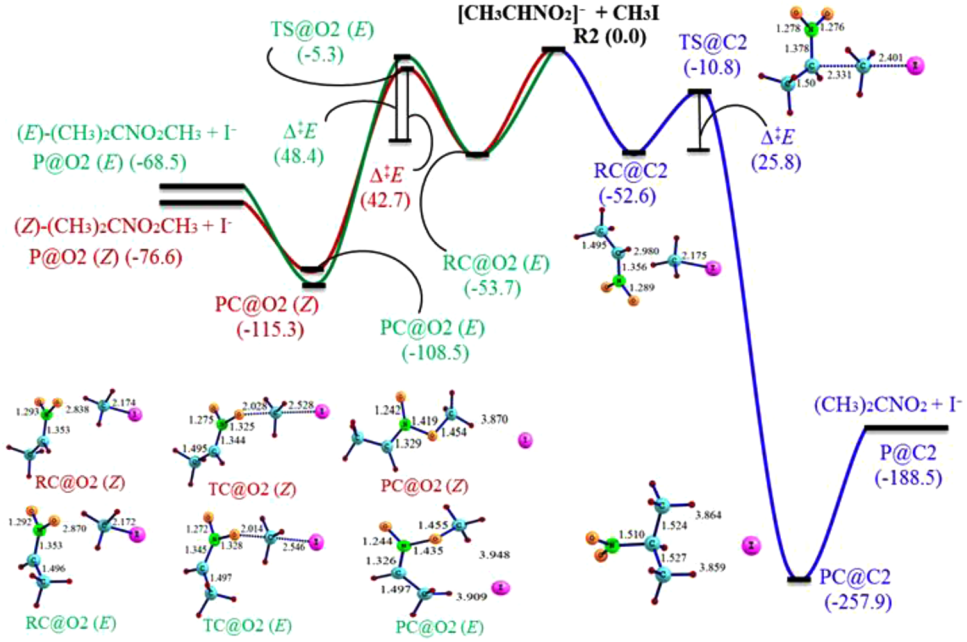

Figure 2. Same as Figure 1 for the $[CH_3CHNO_2]^-$ + CH_3I reaction of **2**.

The experimental kinetic measurements provided the following values for the overall rate coefficients:[19] k_{obs}(**1**) = 1.05 × 10^{-10} molecule^{-1} cm^3 s^{-1}, k_{obs}(**2**) = 1.50 × 10^{-10} molecule^{-1} cm^3 s^{-1}, k_{obs}(**3**) = 1.77 × 10^{-10} molecule^{-1} cm^3 s^{-1}, and k_{obs}(**4**) = 5.02 × 10^{-10} molecule^{-1} cm^3 s^{-1}, with an accuracy of ±25%.[19,20] Notice that the reaction rates increase with the crowdedness around the deprotonated carbon atom (carbanion). Thus, it was suggested[19] that O-methylation should be preferred because the steric effects would be insignificant in this pathway. In addition, as mentioned previously, the nitronic esters provided from O-alkylations are the primary products in solution. However, because the neutral products could not be detected and characterized in the experiments, this suggestion about the C/O selectivity of this reaction could not be ascertained. As a result, our main goal consists of studying these reactions in the gas phase with *ab initio* quantum chemical methods to determine the reaction mechanism and to explain its selectivity and reactivity. In fact, we intend to show that the C-methylation is thermodynamically and kinetically preferred, thus contradicting the proposed

DOI: 10.1021/acs.joc.5b01273
J. Org. Chem. 2015, 80, 8198−8205

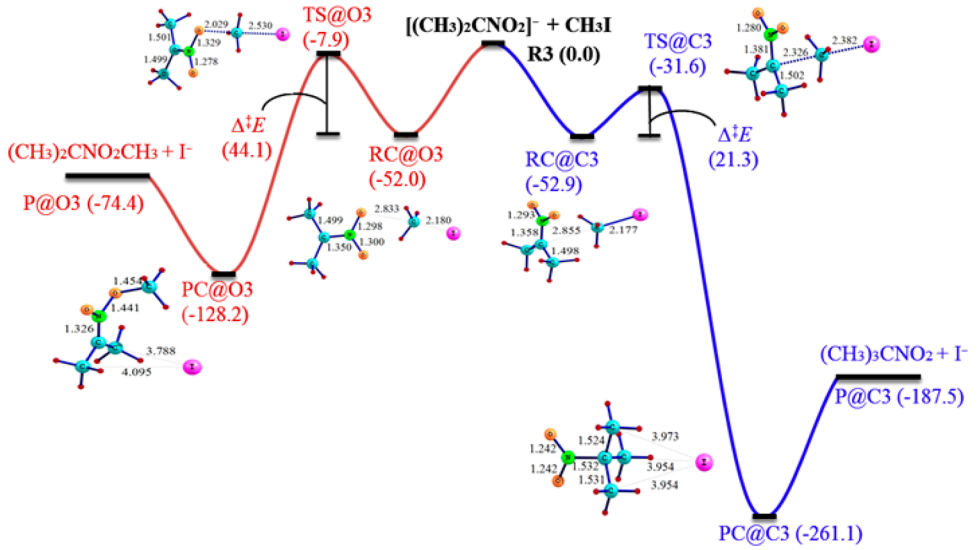

Figure 3. Same as Figure 1 for the $[(CH_3)_2CNO_2]^-$ + CH_3I reaction of **3**.

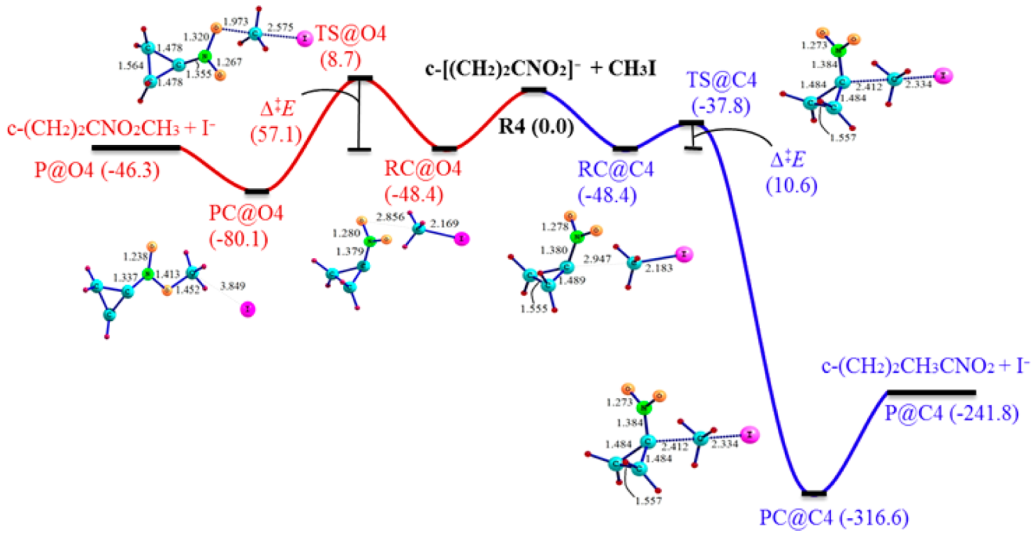

Figure 4. Same as Figure 1 for the $[c\text{-}(CH_2)_2CNO_2]^-$ + CH_3I reaction of **4**.

selectivity. In addition, the reactivity may be explained by the different sp^3 character of the carbanion in the nucleophile (nitronate) and by the vibrational frequencies associated with the pyramidalization of this carbon atom.

RESULTS AND DISCUSSION

Gas-phase S_N2 reactions have been widely explored by computational methods; benchmark assessment studies have shown that the MP2 method with large basis set is the most suitable for kinetic simulations,[21−28] whereas DFT-based methods have performances that may depend upon the particular system.[27,28] Calculations of the enthalpies of deprotonation of nitroalkanes[19] and the vibrational frequencies of CH_3NO_2 were compared with the experimental values[29,30] to ascertain the reliability of MP2 and DFT methods (Tables S1 and S2 of the Supporting Information). Indeed, the overall results provided by the MP2 method with medium to large basis sets are in excellent agreement with the experiment. However, systematic calculations (Tables S3 and S4 of the Supporting Information) of the activation energies of $[R^1R^2CNO_2]^-$ + CH_3I reactions, especially the difference between the nucleophilic replacement through the carbon and the oxygen atoms, showed a strong dependence with the basis set employed. Thus, the energies of the stationary structures of the reaction profiles were extrapolated to the complete basis set limit (CBS) to provide accurate results for kinetic calculations using the RRKM theory. We have also provided comparisons with selected DFT functionals.

Reaction Energy Profiles and Structures. The potential energy profiles of $[R^1R^2CNO_2]^-$ + CH_3I reactions, where R^1 = R^2 = H (**1**), R^1 = CH_3 and R^2 = H (**2**), R^1 = R^2 = CH_3 (**3**), and R^1 + R^2 = c-$(CH_2)_2$ (**4**), calculated at the MP2/CBS level are presented in Figures 1−4. These energy profiles show the typical behavior of a double-well/single-barrier model of S_N2-type reactions[26−28,31,32] involving either the carbon (S_N2@C) or the oxygen (S_N2@O) atom of the nucleophile. Both pathways start at the appropriate reactant complex (RC@C or RC@O) formed between the anion and the polar neutral substrate. These reactant complexes formed at the oxygen are slightly more stable for **1** and **2**, while the reverse is observed for **3**; for **4**, they are degenerate. These results are relevant because they suggest that a pre-equilibration between the

DOI: 10.1021/acs.joc.5b01273
J. Org. Chem. 2015, 80, 8198−8205

reactant complexes should not strongly affect selectivity. Thus, the selectivity should be driven by the kinetics. From the respective reactant complex, the reaction proceeds through a typical bipyramidal distorted transition state structure[21−28,31,32] toward the product, where the structures are also illustrated in Figures 1−4 with selected distances values.

A general feature of these energy profiles is that the C-methylation pathways (S_N2@C) have energy barriers almost half, except for **4**, where this barrier is nearly one-sixth, of that of the corresponding pathway through the oxygen (S_N2@O), O-methylation. Other general and relevant features of these energy profiles are as follows. (i) The activation energies ($\Delta^{\ddagger}E$) of the C-alkylation reactions are as follows: $\Delta^{\ddagger}E(\mathbf{1}) > \Delta^{\ddagger}E(\mathbf{2}) > \Delta^{\ddagger}E(\mathbf{3}) \gg \Delta^{\ddagger}E(\mathbf{4})$. Those of O-alkylation are as follows: $\Delta^{\ddagger}E(\mathbf{4}) \gg \Delta^{\ddagger}E(\mathbf{2}\text{-}Z) \geq \Delta^{\ddagger}E(\mathbf{1}) > \Delta^{\ddagger}E(\mathbf{3}) \geq \Delta^{\ddagger}E(\mathbf{2}\text{-}E)$. The trend observed for the C-methylation reactions follows the same trend of the experimental rate constants. (ii) The reactant complexes (RCs) are formed with an internal energy excess of ~50 kJ mol^{-1}. This suggests that the RCs have enough internal energy to overcome the energy barriers, especially via the S_N2@C pathway. (iii) The product complexes formed through C-methylation (PC@C) are ~140 kJ mol^{-1} more stable than the corresponding PC@O, except for **4**, where this stability is nearly 240 kJ mol^{-1}. The reactions are highly exothermic, especially for the formation of PC@C. These results combined indicate that these gas-phase reactions should be quite efficient and irreversible.

Clearly, considering the difference between the activation energies and the exothermicities, the reaction pathways through the carbon atom are strongly preferred. These results do contradict the proposed explanation for the differences in reaction efficiencies;[19] namely, as the nucleophile becomes more sterically hindered, the reaction efficiencies increase and, thus, the nucleophilic attack should be through the oxygen atom where the steric effect is insignificant. For ring-substituted phenyl-nitronates $[R^1R^2CNO_2]^-$, where R^1 = X-Ph and R^2 = H, B3LYP/6-31+G* calculations provided barriers for O-methylation slightly lower than those of the respective C-methylation.[11] The origin of these differences between alkyl and aryl nitronate regioselectivities is under investigation. Notice that the transition states for O-alkylation (TS@O) of symmetric nitronates are doubly degenerate, and thus, care must be exercised when inferring the selectivity from the energy differences between TS@C and TS@O, except for the O-methylation of **2** that can occur via two different pathways, TS@O (*E*) and TS@O (*Z*), to form isomers *E* and *Z*, respectively (see Scheme 1), which are thus treated separately.

It is noteworthy that the calculated difference in the activation energies between both pathways (TS@C vs TS@O) is directly related to the difference in the exothermicity of the respective product, in accordance with the Bell−Evans−Polanyi principle.[33−35] In other words, we could use the difference in exothermicity to predict selectivity. Employing average bond strengths to estimate reaction enthalpy is not a straightforward task for these reactions because of the Lewis structures associated with the R−NO_2 and C═N(O)O−R groups. For instance, the exothermicity difference between O- and C-methylation $R^1R^2C{=}N(=O){-}O{-}Me \rightarrow R^1R^2C(Me){-}N(=O)_2$ is approximated as $\Delta_r H \approx [L(C{=}N) - L(N{=}O)] + [L(N{-}O) - L(C{-}N)] + [L(C{-}O) - L(C{-}C)] = (615 - 594) + (201 - 305) + (360 - 347) = 21 - 104 + 13 = 70$ kJ mol^{-1}, where L(A−B) are average bond enthalpies.[36] Thus, the greater exothermicities of the C-methylated products are in agreement with the quantum chemical calculations, despite the underestimation of more than twice by the average bond enthalpy approach applied to those Lewis structures. It is noteworthy that the origin of the higher exothermicity of the C-methylated products is the much stronger C−N bond compared to the N−O bond.

With regard to the structures of the main stationary points on the energy profiles, we observed that transition states show the following order of the C−I distance: **1** > **2** > **3** > **4** for the C-methylation (TS@C) and **4** > **2**-*Z* ≥ **1** > **3** ≥ **2**-*E* for the O-methylation (TS@O). These sequences match exactly those observed for their respective activation energies. This is because the C−I distance is associated with the geometry distortion from the reactant structure (positive contribution to the activation energy) and with the partially broken C−I bond (stabilizing contribution to $\Delta^{\ddagger}E$). Namely, the shortest C−I distance would have the smallest distortion and the largest C−I stabilizing interaction, thus, the smallest activation energy. In fact, the trends observed for the C−I distances indicate that the most exothermic reactions (C-methylation) occur through earlier transition states that correlate to lower activation energies for larger reaction exothermicities via the Bell−Evans−Polanyi principle.[33−35]

In a more technical note, we observed that the activation energies of the reaction pathway through the carbon atom decrease more strongly than that through the oxygen atom with an increase in the basis set because the former mechanism involves a larger structural and electronic rearrangement of the nucleophile and should be more susceptible to the quality of the basis set employed (see Table S3 of the Supporting Information). With regard to the reliability and convergence of the calculated properties, the potential energy profiles of methylation reactions of **1** and **2** were determined with the MP2/aug-cc-pVTZ method, which corroborated quantitatively the results presented in Figures 1 and 2, as presented in Tables S4 and S5 of the Supporting Information.

Despite the agreement between observed and calculated trends, a consistent explanation for this reaction mechanism and experimental results is still lacking. This explanation should be based on comparisons between the calculated rate constants and kinetic simulations as well as the origin of the reactivity differences. We thus present next the results for the RRKM calculations of the rate constants, the numerical solutions of the complete kinetic scheme of these reactions, and the possible reasons for the observed and calculated dependence of the nucleophile reactivity upon substituent replacements.

Reaction Rates and Kinetic Simulations. To calculate the relative concentrations and, thus, the reaction selectivity, we solved the kinetic rate equations, which depend upon the rate constant of each elementary step. Scheme 2 represents all of the different pathways of the reaction between iodomethane and nitroalkane anions (nitronates).

Simulations of the kinetics of these reactions require the knowledge of the rate constants associated with the reactant complexes, their reactions to form the product complexes that dissociate into the products. Because the reactions are highly exothermic, the backward rate constants (k_{31}, k_{41}, k_{53}, k_{64}, k_{75}, and k_{86}) are very small. The capture rate constants for the formation of the reactant ion−dipole complexes (k_{13} and k_{14}) and product ion−dipole complexes (k_{75} and k_{86}) were calculated within the parametrized average dipole orientation (ADO) theory.[37−42] This choice of theory was predicated upon the consistency with the experimental measurements and

DOI: 10.1021/acs.joc.5b01273
J. Org. Chem. 2015, 80, 8198−8205

Scheme 2. Kinetic Scheme for the S_N2 Reaction Pathways Involving Deprotonated Nitroalkane (nitronate) Nucleophiles (Nuc) and Iodomethane Substrate (R)

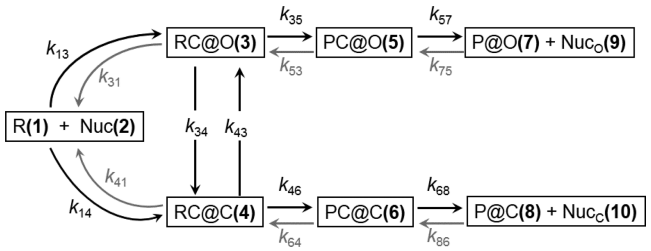

calculations of the reaction efficiencies. Using the MP2/aug-cc-pVDZ calculated dipole moment and polarizability of the neutral substrate (CH_3I) for reactant complexes and those of the neutral products (P@C and P@O) for product complexes, the values of $k_{13} = k_{14}$ of k_{75} and k_{86} were obtained (Tables S6 and S7 of the Supporting Information). The dissociation rate constants of the reactant complexes (k_{31} and k_{41}) were estimated from the equilibrium constant obtained from the calculated standard Gibbs free energy, and similarly for the dissociation rates of the product complexes. The remaining rate constants were obtained by integration of the microcanonical RRKM rates[43−45] weighted by the Boltzmann factor at 298 K.[45] In the RRKM theory,[43−45] the structures and vibrational frequencies calculated at the MP2/aug-cc-pVDZ level were employed, whereas the energy barriers were provided by the MP2/CBS method. The available energy (E) to be distributed within the rovibrational states is given by $E_0 + E_{thermal}$, where E_0 is calculated as the difference between the energies of the transition state and the separated reactants while $E_{thermal}$ is the (classical) thermal energy.[43−45] The calculated canonical rate constants for each reaction pathway are presented in Figures 5

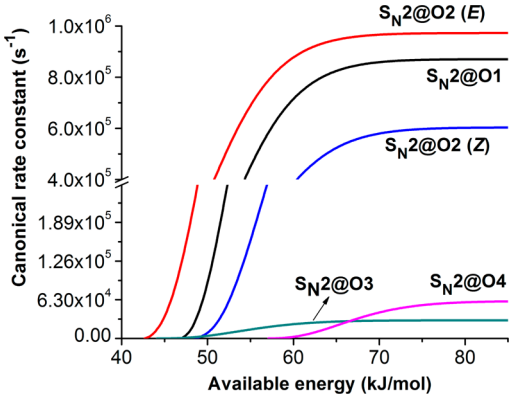

Figure 5. Canonical rate constants for the O-methylation (@O) of the nitronates $[H_2CNO_2]^-$ (**1**), $[CH_3CHNO_2]^-$ (**2**), $[(CH_3)_2CNO_2]^-$ (**3**), and $[c\text{-}(CH_2)_2CNO_2]^-$ (**4**) with CH_3I, calculated with the RRKM theory as a function of the available energy to the reactant complexes, starting at the E_0.

and 6. It can be observed that the canonical rate constants for the C-methylation reactions have the order **4** > **3** > **1** > **2**, while the O-methylation has the order **2**-*E* > **1** > **2**-*Z* > **4** > **3**, which is not exactly the same sequence as that of the activation energies. Therefore, one can say that the activation energy is not the only determining factor of the reaction rate. However, the calculated trend for the C-methylation reactions does coincide with the observed reaction rates; namely, k_{obs} (10^{-10}

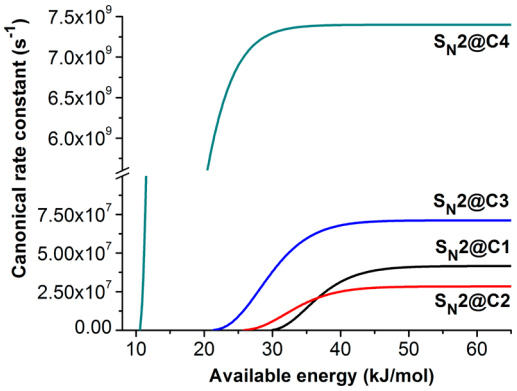

Figure 6. Same as Figure 5 for the C-methylation (@C) of the nitronates.

molecule^{-1} cm^3 s^{-1}) = 1.05, 1.50, 1.77, and 5.02 for nitronates **1**−**4**, respectively.[19] It also can be observed in Figure 6 that the canonical rate constant of C-methylation reaction of **2** is initially larger than that of reaction of **1**. However, as the available energy increases, the rate of **1** becomes higher than that of **2**, because the reactant complex of **1** has fewer vibrational modes than that of **2**. Therefore, the available energy is more focused toward the reaction coordinate for the alkylation of nitronate **1**.

Clearly, despite the O-methylation reactions being doubly degenerate, the regioselectivity toward the formation of the C−C bond is highly preferred according to the canonical rates by several orders of magnitude.

The rate equations associated with the kinetic scheme were solved numerically using the fourth-order Runge−Kutta method with an adaptive integration step.[46] To mimic the experimental conditions,[19] the initial concentration of the nucleophile, Nuc(**2**), was set to 10^4 times smaller than the concentration of the neutral substrate, R(**1**), in Scheme 2. The initial concentrations of the remaining species were set to zero. The temporal dependence of the formation of the product through each reaction pathway is presented in Figure 7.

Once the reactions have reached completion, the O:C product ratio can be calculated for each nitronate to provide quantitative measurements of selectivity. Notice that this

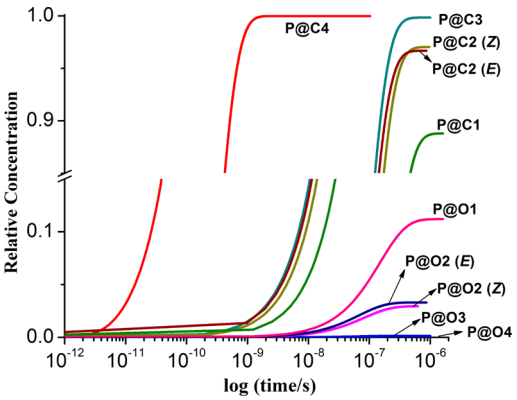

Figure 7. Temporal dependence of the relative concentration of the O-methylation (@O) and C-methylation (@C) products of nitronates $[H_2CNO_2]^-$ (**1**), $[CH_3CHNO_2]^-$ (**2**), $[(CH_3)_2CNO_2]^-$ (**3**), and $[c\text{-}(CH_2)_2CNO_2]^-$ (**4**) by CH_3I, at available energy $E_0 + E_{thermal}$. This simulation uses the equilibrium between the reactant complexes, namely, $k_{34} \cong k_{43} \sim 10^{12}$ s^{-1}, $k_{31} \neq 0$, and $k_{41} \neq 0$.

DOI: 10.1021/acs.joc.5b01273
J. Org. Chem. 2015, 80, 8198−8205

selectivity will depend upon the values of the interconversion rates between the reactant complexes, namely, k_{34} and k_{43}. Thus, when $k_{34} = k_{43} = 0$, we have no equilibrium between the reactant complexes, which represents a purely kinetic control of selectivity, whereas for k_{34} and k_{43} obtained from the RRKM theory that provides values on the order of 10^{12} s^{-1}, a pre-equilibrium is established between the reactant complexes and the concentration of the slower pathway can populate the faster one. We also can assume that the reactant complexes are not in equilibrium ($k_{34} = k_{43} = 0$) and also not in equilibrium with the separated reactants ($k_{31} = k_{41} = 0$). The selectivities for all these cases are listed in Table 1. When the reaction pathways are

Table 1. C-Methylation:O-Methylation Product Ratios of Nitronates $[R_1R_2CNO_2]^-$ by CH_3I at Different Equilibrium Situations between the Reactant Complexes[a]

nitronate	$k_{34} = k_{43} = 0$	$k_{34} \cong k_{43} \sim 10^{12}$ s^{-1}
1	66:34	89:11
2-*E*	61:39	97:03
2-*Z*	70:30	97:03
3	94:06	100:0
4	97:03	100:0

[a]Calculations at available energy $E = E_0 + E_{thermal}$.

independent ($k_{34} = k_{43} = 0$; $k_{31} = k_{41} = 0$), there is no selectivity because the reactant complexes RC@O and RC@C are formed at the same rate ($k_{13} = k_{14}$), except for nitronate **4**, $[c\text{-}(CH_2)_2CNO_2]^-$, for which the rate of dissociation of the reactant complex is so small that the RC@O species becomes trapped and yields a C-methylation:O-methylation ratio of 50:23 on the time scale of the simulation. If the reactant complexes are allowed to dissociate back to the separated reactants (k_{31} and $k_{41} \neq 0$), then some selectivity toward the C-methylation is observed. Indeed, in this case, when these back-dissociation rates become comparable to the rates of the RC → PC steps, the C-methylation selectivity increases significantly because it is the fastest reaction pathway. In the limit where the reactant complexes RC@O and RC@C are in fast pre-equilibrium, the C-methylation is dominant and practically quantitative.

In flowing afterglow studies, as already mentioned, the concentration of the neutral substrate, [R], is ~10^4 times larger than the anion (nucleophile) concentration, [Nuc], typically [R] ~ 10^{12} molecules cm^{-3} and [Nuc] ~ 10^8 molecules cm^{-3}.[19,20] Thus, the pseudo-first-order kinetics applies, and the bimolecular reaction rate coefficient can be estimated with an accuracy of ±25%.[19,20] The numerical simulations of the kinetic mechanisms (Scheme 2) provide the temporal dependence of the concentration of each species for both reaction pathways, which can be used to obtain the overall rate coefficient (k_{obs}) for comparison with the experimental value. In fact, plots of $\ln[RC]$ or $\ln(1 - [P]/[RC]_0)$ versus time (t) have slopes equal to $[Nuc]k_{obs}$, where [RC] and [P] are the overall concentrations of the reactant complexes and the products at time t, respectively, and [Nuc] is the concentration of the nitronate. Unfortunately, this concentration was not provided in the experimental studies, and direct comparisons with the calculated values are not feasible. Therefore, in Table 2, we present the relative rate coefficients calculated for the three cases considered as well as the experimental values.

The trend in the calculated relative rate coefficients considering the equilibrium between the reactants and reactant

Table 2. Calculated and Experimental Relative Rate Coefficients for the $[R^1R^2CNO_2]^-$ + CH_3I Gas-Phase Reactions[a]

nitronate	$k_{31} = k_{41} = 0$; $k_{34} = k_{43} = 0$	$k_{34} = k_{43} = 0$	$k_{34} \cong k_{43}$[b]	experiment[19]
1	1.0	1.0	1.0	1.0
2-*E*	0.7	0.7	2.2	1.4
2-*Z*	0.7	0.7	1.8	
3	1.8	1.6	2.3	1.7
4	174	189	670	4.8

[a]Calculations at available energy $E = E_0 + E_{thermal}$. Relative rate coefficients: $k_{obs}/k_{obs}(\mathbf{1})$. [b]Approximately 10^{12} s^{-1}.

complexes (fourth column in Table 2) matches the experimental one. This is consistent with the experimental conditions under which the kinetic measurements are performed in buffer gas (helium) at 40 Pa, which could allow the equilibrium between the reactant complexes to be reached. These trends show that the bimolecular reaction rate coefficients increase with the increase in crowdedness around the central carbon atom of the nitronate. However, the calculations do overestimate the substituent effects on the reaction rates, especially of nitronate **4**, $[c\text{-}(CH_2)_2CNO_2]^-$. These overestimations may be due to dynamics effects[26,27] that are not taken into consideration in the RRKM calculations as well as electron correlation effects on the activation energies. For instance, reactions between methyl nitrate (CH_3ONO_2) and OH^- can occur via the S_N2 direct mechanism without forming the reactant complex.[27] In addition, for these reactions, the long-range electrostatic interactions can direct the nucleophilic attack and determine the selectivity.[27] Another relevant dynamics effect is the significant number of quasiclassical trajectories that present recrossings during S_N2 pathways.[26,27] Therefore, for quantitative predictions of the relative and absolute rate coefficients of the $[R^1R^2CNO_2]^-$ + CH_3I gas-phase reactions, the inclusion of dynamics effects via, for instance, quasiclassical direct molecular simulations, is probably necessary.

Explaining the Selectivity and Reactivity. The agreement between the calculated and experimental trends suggests that the theoretical approach is reliable and may be used to explain the dependence of the rate coefficients on the nitronates. Indeed, the increase in the rate coefficients with the increase in crowdedness around the central carbon atom of the nucleophile suggested selectivity toward the O-methylation of the nitronate.[19] However, the calculated energy profiles showed a high regioselectivity toward C-methylation, which is corroborated by the agreement between the experimental and calculated trends of the reaction rates. The explanation for this regioselectivity can be drawn from the Bell−Evans−Polanyi principle, where the most exothermic pathway (C-methylation) should be preferred because it would have a smaller activation energy. The differences in the exothermicity of C- and O-alkylated products were already qualitatively rationalized in terms of average bond enthalpies.

A complete explanation still needs to account for the increase in the reaction rate coefficients upon the increase in the substituents at the central carbon atom of the nitronate. The structures of nucleophiles **1**−**3** are planar, whereas nitronate **4** presents a pyramidal geometry around the central carbon. This suggests that this central carbon should have a strong sp^2 character in nucleophiles **1**−**3**, while sp^3 hybridization would be

DOI: 10.1021/acs.joc.5b01273
J. Org. Chem. 2015, 80, 8198−8205

expected in nucleophile **4**. Because this carbon atom has sp^3 hybridization in the products, the largest reaction rate coefficient obtained with nitronate **4** may be explained by the smaller energy required to deform its electronic density from the reactant to the product. The same rationale suggests that the degree of sp^3 hybridization at the central carbon atom of the nucleophile would be related to the increase in the reaction rates. The barriers to internal rotation of the C−N bond in the nitronate and in the product were used to infer the degree of sp^3 hybridization. The differences between these barriers are 125.2, 139.5, and 132.8 kJ mol^{-1} for nitronates **1**−**3**, respectively. Notice that these differences do not explain the observed reactivity of these nucleophiles. Analyses using electron density and orbitals[47,48] have provided inconclusive results for the hybridization character at the central carbon atom. However, vibrational analysis showed that the frequency of the normal mode related to the pyramidalization of the central carbon decreases significantly in the series of **1**, **2**, and **3**, as observed in Table 3. This trend matches perfectly the calculated and experimental trends in reactivity. In fact, the decrease in this vibrational frequency upon the increase in substituents is directly related to a decrease of the force constant and an increase in the reduced mass, where the former has a larger effect. Steric effects between the substituents at the central carbon atom are probably the reason for the significant decrease in the force constant in the series of **1**, **2**, and **3**. Thus, thermal excitation of this low-frequency mode is more likely, which causes the reaction to accelerate because the nitronate would be more apt to react. In fact, because this normal mode can couple with the intermolecular mode of the S_N2 pathway,[26,27,31,32] the direct mechanism without the formation of the reactant complexes also becomes more probable as the frequency of the pyramidalization mode decreases.

Table 3. Vibrational Properties of the Central Carbon Pyramidalization Mode of the Nucleophiles Calculated with the MP2/aug-cc-pVDZ Method[a]

	1	2	3	4
ν	326	155	87	228
k	7.88	4.85	0.68	10.87
μ	1.26	4.08	1.53	3.53

[a]Vibrational frequency ν (cm^{-1}), force constant k (N m^{-1}), and reduced mass μ (amu).

CONCLUSIONS

Methylation of deprotonated alkyl-nitroalkanes or nitronates, $[R^1R^2CNO_2]^-$, where $R^1 = R^2 = H$ (**1**), $R^1 = CH_3$ and $R^2 = H$ (**2**), $R^1 = R^2 = CH_3$ (**3**), and $R^1 + R^2 = c\text{-}(CH_2)_2$ (**4**), by CH_3I in the gas phase was successfully modeled by the MP2/CBS method. The C- and O-methylation regioselectivity and the reactivity of these nitronates were studied. The experimental rate coefficients (k_{obs}) follow the trend **1** (1.0) < **2** (1.4) < **3** (1.7) ≪ **4** (4.8),[19] where the values in parentheses are relative rate coefficients $k_{obs}/k_{obs}(\mathbf{1})$. It was thus proposed[19] that the alkylation should proceed through the oxygen atom of the nitronate, to account for the increase in the steric effect around the carbanion. The quantum chemical calculations showed that the C-methylation would be preferred because they presented significantly smaller activation energies. Indeed, the selectivity toward the C-alkylated products and the reactivity trend **4** ≫ **3** > **2** > **1** were quantitatively ascertained by RRKM calculations of the rate constants and numerical simulations of the kinetic equations. The selectivity may be explained by the much larger exothermicity of the C-methylation compared to that of O-methylation, according to the Bell−Evans−Polanyi principle. These higher exothermicities can be qualitatively obtained using average bond enthalpies of appropriate Lewis structures. The reactivity of **4** being much larger than those of the other nucleophiles was explained by the already large sp^3 character of the carbanion in nucleophile **4**, whereas the reactivity trend **3** > **2** > **1** could be explained by the significant increase in the vibrational frequency associated with the pyramidalization mode in this series.

Because the O-methylation of nitronate **2** with trialkyloxonium is preferred in solution,[49] the origin of the regioselectivity of alkylation of nitronates in solution needs to be revisited,[11] where the solvent effects as well as the alkylating agent may play decisive roles, which could provide new design strategies for controlling these reactions.

COMPUTATIONAL SECTION

All electronic structure simulation calculations were performed with the Gaussian 09 program[50] using its default criteria. Molecular structures were determined without symmetry constraints with the MP2[51,52] method using aug-cc-pVDZ and aug-cc-pVTZ basis sets.[53−56] The extrapolation to the complete basis set (CBS) limit was performed from MP2/aug-cc-pVXZ (X = D, T, and Q) energy calculations.[57,58] Optimized structures with all positive force constants were characterized as stable species, whereas those having all but one positive force constant were transition states. Intrinsic reaction coordinate (IRC) calculations were performed to properly connect the transition state to its respective reactant and product complexes. RRKM calculations[43−45] were conducted for energy values (E) from E_0 to $E_0 + E_{thermal}$ (at 298 K) using the superRKKM program.[59] The initial value E_0 was taken as the complexation energy of RC. The RRKM rate constants $k_a(E)$ were weighted by a Boltzmann distribution and integrated from E_0 to $E_0 + E_{thermal}$ to yield the canonical rate constant at 298 K. The numerical solution of the coupled differential equations describing the kinetic scheme was obtained using an in-house program employing the fourth-order Runge−Kutta method with an adaptive integration step.[46] The initial concentrations of the nitronate and the neutral substrate were 1 and 10^4, respectively, with the initial time step set to 10^{-16} s.

ASSOCIATED CONTENT

Supporting Information

Additional tables and figures for comparisons and Cartesian coordinates of all stationary points in the potential energy profiles. The Supporting Information is available free of charge on the ACS Publications website at DOI: 10.1021/acs.joc.5b01273.

AUTHOR INFORMATION

Corresponding Authors

*E-mail: ayyazcmc@gmail.com.
*E-mail: longo@ufpe.br.

Notes

The authors declare no competing financial interest.

ACKNOWLEDGMENTS

The Brazilian Agencies CNPq, CAPES, FACEPE, and FINEP are acknowledged for providing financial support under Grants Pronex APQ-0859-1.06/08 and INCT-INAMI Proc. no. 573986/2008-8. A.M. thanks CNPq for graduate scholarship,

DOI: 10.1021/acs.joc.5b01273
J. Org. Chem. 2015, 80, 8198−8205

and E.S.T. thanks PNPD/FACEPE-CAPES for a post-doc fellowship.

REFERENCES

(1) Breuer, E.; Aurich, H. G.; Nielsen, A. In *Nitrones, Nitronates and Nitroxides: The Chemistry of Functional Groups*; Patai, S., Rappoport, Z., Eds.; John Wiley & Sons: New York, 1989; Chapter 3.
(2) Noboro, O. In *The Nitro Group in Organic Synthesis*; Wiley-VCH: New York, 2001.
(3) Rosini, G. In *Comprehensive Organic Synthesis*; Trost, B. M., Ed.; Pergamon: New York, 1991; Vol. 2.
(4) Fever, H., Nielsen, A. T., Eds. *Nitro Compounds, Recent Advances in Synthesis and Chemistry*; VCH: Weinheim, Germany, 1990.
(5) Ioffe, S. L.; Zelinsky, N. D. In *Nitrile Oxides, Nitrones and Nitronates in Organic Synthesis: Novel Strategies in Synthesis*, 2nd ed.; Feuer, H., Ed.; 2008; Chapter 3, pp 435−748.
(6) Kurti, L.; Czako, B. In *Strategic Applications of Named Reactions in Organic Synthesis*; Elsevier Academic Press: Burlington, MA, 2005.
(7) Denmark, S. E.; Cottell, J. J. In *Synthetic Applications of 1,3-Dipolar Cycloaddition Chemistry Toward Heterocycles and Natural Products*; Padwa, A., Pearson, W. H., Eds.; John Wiley & Sons, Inc.: New York, 2002; Vol. *59*, Chapter 2, pp 83−167.
(8) Torssell, K. B. G. In *Nitrile Oxides, Nitrones, and Nitronates in Organic Syntheis*; VCH Publishers: New York, 1988.
(9) Lecea, B.; Arrieta, A.; Morao, I.; Cossio, F. P. *Chem. - Eur. J.* **1997**, *3*, 20−28.
(10) Linton, B. R.; Goodman, M. S.; Hamilton, A. D. *Chem. - Eur. J.* **2000**, *6*, 2449−2455.
(11) Sakata, T.; Seki, N.; Yomogida, K.; Yamagishi, H.; Otsuki, A.; Inoh, C.; Yamataka, H. *J. Org. Chem.* **2012**, *77*, 10738−10744.
(12) Garver, J. M.; Fang, Y.-r.; Eyet, N.; Villano, S. M.; Bierbaum, V. M.; Westaway, K. C. *J. Am. Chem. Soc.* **2010**, *132*, 3808−3814.
(13) Chandrasekhar, J.; Smith, S. F.; Jorgensen, W. L. *J. Am. Chem. Soc.* **1985**, *107*, 154−163.
(14) Bohme, D. K.; Mackay, G. I. *J. Am. Chem. Soc.* **1981**, *103*, 978−979.
(15) Bohme, D. K.; Rakshit, A. B.; Mackay, G. L. *J. Am. Chem. Soc.* **1982**, *104*, 1100−1101.
(16) Brauman, J. I.; Blair, L. K. *J. Am. Chem. Soc.* **1970**, *92*, 5986−5987.
(17) Taft, R. W. *Prog. Phys. Org. Chem.* **1983**, *14*, 247−350.
(18) Olmstead, W. N.; Brauman, J. I. *J. Am. Chem. Soc.* **1977**, *99*, 4219−4228.
(19) Kato, S.; Carrigan, K. E.; DePuy, C. H.; Bierbaum, V. M. *Eur. Mass Spectrom.* **2004**, *10*, 225−231.
(20) Bierbaum, V. M.; DePuy, C. H.; Shapiro, R. H.; Stewart, J. H. *J. Am. Chem. Soc.* **1976**, *98*, 4229−4235.
(21) Gronert, S. *J. Am. Chem. Soc.* **1991**, *113*, 6041−6048.
(22) Merrill, G. N.; Gronert, S.; Kass, S. R. *J. Phys. Chem. A* **1997**, *101*, 208−218.
(23) Bento, A. P.; Solà, M.; Bickelhaupt, F. M. *J. Chem. Theory Comput.* **2008**, *4*, 929−940.
(24) Pabis, A.; Paluch, P.; Szala, J.; Paneth, P. *J. Chem. Theory Comput.* **2009**, *5*, 33−36.
(25) Zhao, Y.; Truhlar, D. G. *J. Chem. Theory Comput.* **2010**, *6*, 1104−1108.
(26) Manikandan, P.; Zhang, J.; Hase, W. L. *J. Phys. Chem. A* **2012**, *116*, 3061−3080.
(27) de Souza, M. A. F.; Correra, T. C.; Riveros, J. M.; Longo, R. L. *J. Am. Chem. Soc.* **2012**, *134*, 19004−19010.
(28) Proenza, Y. G.; de Souza, M. A. F.; Ventura, E.; do Monte, S. A.; Longo, R. L. *Phys. Chem. Chem. Phys.* **2014**, *16*, 26769−26778.
(29) Bodenbinder, M.; Ulic, S. E.; Willner, H. *J. Phys. Chem.* **1994**, *98*, 6441−6444.
(30) Maksyutenko, P.; Muzangwa, L. G.; Jones, B. M.; Kaiser, R. I. *Phys. Chem. Chem. Phys.* **2015**, *17*, 7514−7527.
(31) Hase, W. L. *Science* **1994**, *266*, 998−1002.
(32) Chabinyc, M. L.; Craig, S. L.; Regan, C. K.; Brauman, J. I. *Science* **1998**, *279*, 1882−1886.
(33) Bell, R. P. *Proc. R. Soc. London, Ser. A* **1936**, *154*, 414−429.
(34) Evans, M. G.; Polanyi, M. *Trans. Faraday Soc.* **1936**, *32*, 1333−1360.
(35) Anslyn, E. V.; Dougherty, D. A. In *Modern Physical Organic Chemistry*; University Science: Sausalito, CA, 2006.
(36) House, J. E. In *Inorganic Chemistry*; Academic Press: New York, 2008; p 130.
(37) Su, T.; Bowers, M. T. *Int. J. Mass Spectrom. Ion Phys.* **1973**, *12*, 347−356.
(38) Su, T.; Bowers, M. T. *Gas Phase Ion Chemistry*; Academic Press: New York, 1979; Vol. *1*, p 83.
(39) Chesnavich, W. J.; Su, T.; Bowers, M. T. *J. Chem. Phys.* **1980**, *72*, 2641−2655.
(40) Su, T.; Chesnavich, W. J. *J. Chem. Phys.* **1982**, *76*, 5183−5185.
(41) Su, T. *J. Chem. Phys.* **1985**, *82*, 2164−2165.
(42) Su, T. *J. Chem. Phys.* **1994**, *100*, 4703−4703.
(43) Baer, T.; Hase, W. L. In *Unimolecular Reaction Dynamics Theory and Experiments*; Oxford University Press: New York, 1996.
(44) Holbrook, K. A.; Pilling, M. J.; Robertson, S. H. In *Unimolecular reactions*, 2nd ed.; Wiley: New York, 1996.
(45) Henriksen, N. E.; Hansen, F. Y. In *Theories of Molecular Reaction Dynamics: The Microscopic Foundation of Chemical Kinetics*; Oxford University Press: New York, 2008.
(46) Press, W. H.; Flannery, B. P.; Teoukolsky, S. A.; Vetterling, W. T. In *Numerical Recipes: The Art of Scientific Computing*; Cambridge University Press: New York, 1990.
(47) Weinhold, F.; Landis, C. R. In *Discovering Chemistry with Natural Bond Orbitals*; John Wiley & Sons: Hoboken, NJ, 2012.
(48) Cramer, C. J. In *Essentials of Computational Chemistry: Theories and Models*, 2nd ed.; Wiley: New York, 2004.
(49) Kornblum, N.; Brown, R. A. *J. Am. Chem. Soc.* **1964**, *86*, 2681−2687.
(50) Frisch, M. J.; Trucks, G. W.; Schlegel, H. B.; Scuseria, G. E.; Robb, M. A.; Cheeseman, J. R.; Scalmani, G.; Barone, V.; Mennucci, B.; Petersson, G. A.; Nakatsuji, H.; Caricato, M.; Li, X.; Hratchian, H. P.; Izmaylov, A. F.; Bloino, J.; Zheng, G.; Sonnenberg, J. L.; Hada, M.; Ehara, M.; Toyota, K.; Fukuda, R.; Hasegawa, J.; Ishida, M.; Nakajima, T.; Honda, Y.; Kitao, O.; Nakai, H.; Vreven, T.; Montgomery, J. A., Jr.; Peralta, J. E.; Ogliaro, F.; Bearpark, M.; Heyd, J. J.; Brothers, E.; Kudin, K. N.; Staroverov, V. N.; Kobayashi, R.; Normand, J.; Raghavachari, K.; Rendell, A.; Burant, J. C.; Iyengar, S. S.; Tomasi, J.; Cossi, M.; Rega, N.; Millam, J. M.; Klene, M.; Knox, J. E.; Cross, J. B.; Bakken, V.; Adamo, C.; Jaramillo, J.; Gomperts, R.; Stratmann, R. E.; Yazyev, O.; Austin, A. J.; Cammi, R.; Pomelli, C.; Ochterski, J. W.; Martin, R. L.; Morokuma, K.; Zakrzewski, V. G.; Voth, G. A.; Salvador, P.; Dannenberg, J. J.; Dapprich, S.; Daniels, A. D.; Farkas, Ö.; Foresman, J. B.; Ortiz, J. V.; Cioslowski, J.; Fox, D. J. *Gaussian 09*, revision D.01; Gaussian Inc.: Wallingford, CT, 2009.
(51) Hehre, W. J.; Radom, L.; Schleyer, P. v. R.; Pople, J. A. In *Ab Initio Molecular Orbital Theory*; Wiley-Interscience: New York, 1986.
(52) Helgaker, T.; Jørgensen, P.; Olsen, J. In *Molecular Electronic-Structure Theory*; John Wiley & Sons: New York, 2000.
(53) Dunning, T. H., Jr. *J. Chem. Phys.* **1989**, *90*, 1007−1023.
(54) Kendall, R. A.; Dunning, T. H., Jr.; Harrison, R. J. *J. Chem. Phys.* **1992**, *96*, 6796−806.
(55) Woon, D. E.; Dunning, T. H., Jr. *J. Chem. Phys.* **1993**, *98*, 1358−1371.
(56) Woon, D. E.; Dunning, T. H., Jr. *J. Chem. Phys.* **1994**, *100*, 2975−2988.
(57) Truhlar, D. G. *Chem. Phys. Lett.* **1998**, *294*, 45−48.
(58) Halkier, A.; Helgaker, T.; Jørgensen, P.; Klopper, W.; Koch, H.; Olsen, J.; Wilson, A. K. *Chem. Phys. Lett.* **1998**, *286*, 243−252.
(59) Pradie, N. A.; Linnert, H. V. *SuperRRKM*, version 1.0; University of São Paulo: São Paulo, Brazil, 2009.

DOI: 10.1021/acs.joc.5b01273
J. Org. Chem. 2015, 80, 8198−8205